JOURNAL OF MATERIALS SCIENCE 19 (1984) 3806–3813

Some electrical properties of the defective γ phases of spinel structure during their transformation to the rhombohedral α phases

B. GILLOT, R. M. BENLOUCIF, F. JEMMALI
Laboratoire de Recherches sur la Réactivité des Solides, Associé au C.N.R.S., B.P. 138, 21004, Dijon Cedex, France

During the transformation of "cubic" iron sesquioxides, γ-Fe_2O_3, substituted by divalent or trivalent ions, to rhombohedral α phases, the electrical conductivity yields discontinuities and a change in plots of log σ against $f(1/T)$. The average temperature of these discontinuities is influenced by the particle size, and extent of oxidation and substitution. For divalent substituted defective spinels, the activation energy for the haematite precipitation appears to depend on the extent of substitution and the size of the particle.

1. Introduction

Close-packed oxides containing Fe^{2+} ions and corresponding to the formula $(Fe_{3-x}M_x)O_4$ can be oxidized at low temperature ($<300^\circ$ C) to defective γ phases of the same structure for crystallite sizes less than about 300 nm. This is the case for several fine-grained magnetites substituted by trivalent or divalent ions for which the formation of defect spinels has been observed [1]. Moreover, all these γ compounds undergo crystal structure changes with rising temperature [2, 3]; in all cases it is the transformation of a lattice of cubic symmetry into an α rhombohedral lattice which is stable at high temperature. This stability, for example the activation energy of the transition as well as the transition temperature itself, is strongly influenced by the method of preparation, particle size [4], oxidation extent of the initial phase [5], composition and nature of cations present [6].

While establishing the experimental conditions for the γ-$Fe_2O_3 \rightarrow \alpha$-$Fe_2O_3$ transformation at a constant heating rate, an inflection point in the log $\sigma = f(1/T)$ curves (σ being the direct current electrical conductivity) was observed near the transformation temperature [5]. This paper reports a detailed analysis of this type of behaviour in order to determine the effects of crystallite size, oxidation extent and substituents on the relative stability of the defect spinel structure. The kinetics of α-phase precipitation is also studied by electrical conductivity. Interest in this technique has recently been shown for studying the effects of additives and mechanical treatment on the transformation of γ-Fe_2O_3 to α-Fe_2O_3 and for determining the behaviour of γ-Fe_2O_3 in a reducing gas atmosphere [7].

2. Samples and experimental procedure

2.1. Preparation of samples

The techniques of preparation and characterization (DTA, X-ray analysis, morphology, chemical analysis) have already been presented [8–10]. The products oxidized into defective γ phases of the same composition and morphology as the initial products are those obtained by low-temperature oxidation (350° C) of aluminium- or chromium-substituted magnetites $(Fe^{2+}Fe^{3+}_{2-x}M^{3+}_x)O^{2-}_4$ with $0 < x < 2$, as well as mixed ferrites $(Fe^{2+}_{1-x}M^{2+}_xFe^{3+}_2)O^{2-}_4$ with $M^{2+} = Co^{2+}$, Zn^{2+}, Mn^{2+} and $0 < x < 1$ according to the reactions:

$$2(Fe^{2+}Fe^{3+}_{2-x}M^{3+}_x)O^{2-}_4 + 1/2O^{2-}_2 \rightarrow 3(Fe^{3+}_{1-y}M^{3+}_y)_2O^{2-}_3 \quad 0 < y < 2/3$$

and

$$(Fe^{2+}_{1-x}M^{2+}_xFe^{3+}_2)O^{2-}_4 + 1/4(1-x)O^{2-}_2 \rightarrow x(M^{2+}Fe^{3+}_2O^{2-}_4), 3/2(1-x)Fe^{3+}_2O^{2-}_3.$$

For manganese ferrite, X-ray analysis indicated that the Mn^{2+} ion is also oxidized conducting to the defective phase $(Fe_{2-z/3}Mn_{z/3})O^{2-}_3$ with $0 < z < 2$. The defective γ phases were completely converted to rhombohedral α phases by

0022–2461/84 $03.00 + .12

heating above 850° C with the same composition for the phases containing aluminium, chromium or manganese [2] and with haematite precipitation α-Fe_2O_3 and formation of ferrite where M is a divalent cation such as cobalt or zinc [6].

2.2. Measurement of electrical properties

The electrical properties of defective γ phases, of the $\gamma \rightarrow \alpha$ transformation and the kinetics of the precipitation were studied by measuring the direct current (d.c.) electrical conductivity on compressed pellets (diameter 0.8 cm, thickness 2.5 mm) between two spring-located platinum electrodes as reported by Gillot and Ferriot [11]. The pellets were sintered at 850° C for 1 h in a vacuum ($\sim 1 \times 10^{-6}$ atm). The sintered samples thus obtained were differently heat-treated in the cell.

1. In order to determine the behaviour of the electrical conductivity of a sample during oxidation from initial phase to γ, the initial phase was heated in air at a constant rate of 2.5° C min^{-1} from room temperature to 950° C.

2. The samples were heated at 300° C for 20 h in air, during which the initial phase was oxidized to γ. The samples thus obtained were heated at a constant rate from 200 to 950° C.

3. Many experiments were carried out to study the transformation of the partially oxidized γ compound to the rhombohedral α phase. The experimental conditions in which the γ composition of the solid phase in the initial phase will be uniform and oxidation partial, were similar to that reported previously [5]. For example, by oxidizing Fe_3O_4 at 250° C by circulating a mixture of $N_2 + O_2$ gas of given composition previously established in a microbalance [5], an intermediate solid solution between Fe_3O_4 and γ-Fe_2O_3 can be obtained expressed as follows:

$$Fe^{3+}(\square_{\delta}Fe^{2+}_{1-3\delta}Fe^{3+}_{1+2\delta})O^{2-}_4$$

where $\square$ is a cation vacancy, and δ the degree of oxidation ($\delta = 1/3$ when oxidation is total).

3. Results and discussion

3.1. Behaviour of electrical conductivity during transformation of defective γ phases → rhombohedral α phases

3.1.1. Transformation of γ-Fe_2O_3 → α-Fe_2O_3. Influence of crystallite size and oxidation extent

The behaviour of electrical conductivity during transformation from γ-Fe_2O_3 to α-Fe_2O_3 is shown in Fig. 1 in comparison with the DTA curves for samples with a size variation between 60 and 140 nm. In all cases a break is observed in the $\log \sigma = f(1/T)$ curves. For temperatures lower than this break (line CD), the electrical conductivity increases with increase in temperature according to the negative temperature coefficient of γ-Fe_2O_3. At around 450° C, the break (process DE) indicates the transformation from γ to α, because, as shown in Fig. 1, an exothermic peak in the DTA curve is also seen at that temperature. The break is caused by the difference in the temperature dependence of the conductivity between γ-Fe_2O_3 and α-Fe_2O_3 at or near the transformation temperature. The dependence of the electrical conductivity of α-Fe_2O_3 on temperature is illustrated along the process EFG.

In this study, the effect of crystallite size on transformation was directly investigated by evaluating the behaviour of electrical conductivity. If we represent the starting and finishing temperature of the transformation by T_D and T_E, respectively, it was found that a significant shift of T_D and T_E toward higher temperatures was observed with decrease in crystallite size (Fig. 1). The relationships between T_D, T_E, $T_M = (T_D + T_E)/2$ and the crystallite size are given in Table I. The phenomena described above were also observed in the DTA curves. In the present study, a decrease in crystallite size increased the precipitation temperature according to the observations of Egger and Feitknecht [12] and Kimura *et al.* [13]. The result is associated with reduced particle size, which facilitates the release of strain caused by the contraction effects of the lattice during the process of oxidation. As shown in Fig. 2 and Table I, in the case of partially oxidized magnetite (between $\delta = 0.20$ and 0.33), both T_D and T_E increased with increase in the percentage of Fe^{2+} ions. T_D, therefore, rises from 451° C for pure γ-Fe_2O_3 to 545° C for a sample with $\delta = 0.20$. These results indicate that the transformation temperature varies strongly with the fraction of γ-Fe_2O_3 in the Fe_3O_4. Comparing the results from the sample with $\delta = 0.20$ and pure γ-Fe_2O_3 supports the view of Egger and Feitknecht [12] which proposed that α-Fe_2O_3 nuclei are formed as a consequence of the strain induced by the difference in the lattice parameter between unoxidized and oxidized solid solution. X-ray diffraction patterns taken at successive stages of oxidation showed shifts of the diffraction lines

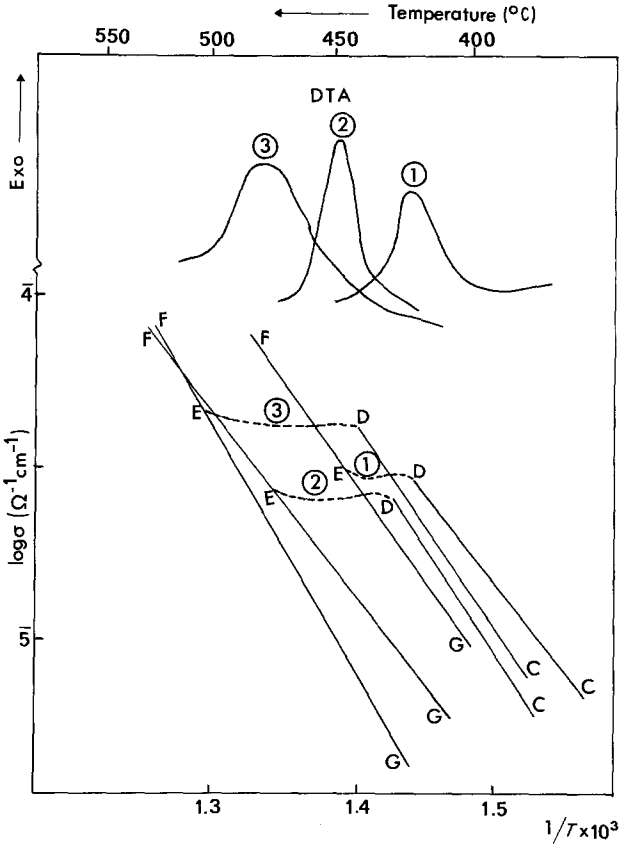

Figure 1 Effect of particle size on the γ-$Fe_2O_3 \rightarrow$ α-Fe_2O_3 transformation and DTA curves: 1, 140 nm; 2, 90 nm; 3, 60 nm.

towards lower d-values concomitant with the contraction of the unit cell, as the amount of γ-Fe_2O_3 in Fe_3O_4 increased, and the nucleation of α-Fe_2O_3 is more difficult for samples with composition $\delta = 0.20$. Moreover, the electrical conductivity of the solid solution (line CD) depends on the amount of Fe^{2+}, that is, the degree of oxidation δ (Fig. 2). The decrease in conductivity with the percentage of Fe^{2+} ions would be attributed to the decrease in the electron exchange process between Fe^{2+} in Fe_3O_4 and Fe^{3+} generated on the grain [10, 14].

3.1.2. Effect of substitution extent during the reaction initial phase $\rightarrow \gamma \rightarrow \alpha$

A plot of $\log \sigma$ against $1/T$ (Fig. 3) of a cobalt-substituted magnetite during oxidation shows the dependence of substitution extent x. In region I, the electrical conductivity of the initial phase decreases with increase in temperature due to the decrease in the amount of Fe^{2+} ions by oxidation until the sample transforms to γ [14]. This decrease is larger in the lower substitution extent than that in the higher extent x, according to the amount of Fe^{2+} initially

TABLE I Evolution of the $\gamma \rightarrow \alpha$ transformation temperature

Fe_2O_3	Particle size (nm)	T_D (°C)	T_E (°C)	$(T_D + T_E)/2$ (°C)	pic ATD (°C)
1	140	421	446	433	426
2	90	429	473	451	449
3	60	441	502	472	489
Fe_3O_4–Fe_2O_3	Degree of oxidation, δ				
2	0.33	429	473	451	449
4	0.28	460	500	483	
5	0.24	490	561	521	
6	0.20	510	600	545	

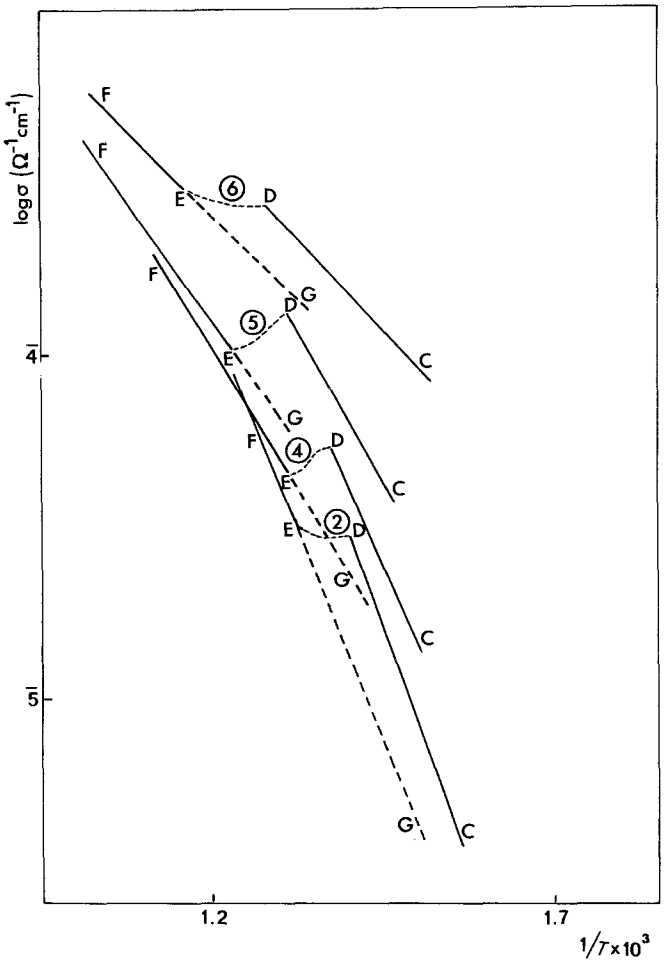

Figure 2 Evolution of electrical conductivity with temperature for different amounts of the γ-phase in the initial phase; Fe_3O_4. 2, $\delta = 0.33$; 4, $\delta = 0.28$; 5, $\delta = 0.24$; 6, $\delta = 0.20$.

present. At the same time the minimum in region I is shifted to lower temperatures. The decrease in σ is then followed by an increase in σ corresponding to complete oxidation to γ (region II), then by a region (III) of roughly linear increase in $\log \sigma$ with T, which is characteristic of the γ-phase. At around 550° C, the $\log \sigma = f(1/T)$ curves show discontinuities, which are represented in dashed lines (region IV). These discontinuities can be regarded as being caused by the transformation $\gamma \rightarrow \alpha$. Table II gives the temperatures T_D and T_E of the beginning and end of each discontinuity, average temperature T_M, related to composition x. A shift in T_M toward higher temperature was observed with increase of substitution extent. The region V is attributed to α-phase as confirmed by X-ray analysis, and during cooling regions IV, III, II and I of the heating curve were not retraced.

When the sample was initially exposed at 300° C to oxygen, the plot of $\log \sigma$ against $1/T$ did not show a rapid decrease in region I (Fig. 3, curve a) since the oxidation is considered to proceed effectively.

3.1.3. Effect of divalent or trivalent cation on transformation

As an example, the behaviour of electrical conductivity near the temperature of transformation is shown in Fig. 4. This behaviour is dependent on divalent or trivalent cations. For instance, in manganese-substituted magnetite the $\gamma \rightarrow \alpha$ transition is marked by a steep increase in σ. A DTA

TABLE II Evolution of the transformation temperature for defective Co-substituted magnetites

Sample x	T_D (° C)	T_E (° C)	$(T_D + T_E)/2 = T_M$ (° C)
0.16	460	502	481
0.42	510	537	523
0.64	534	590	562
0.82	560	614	587

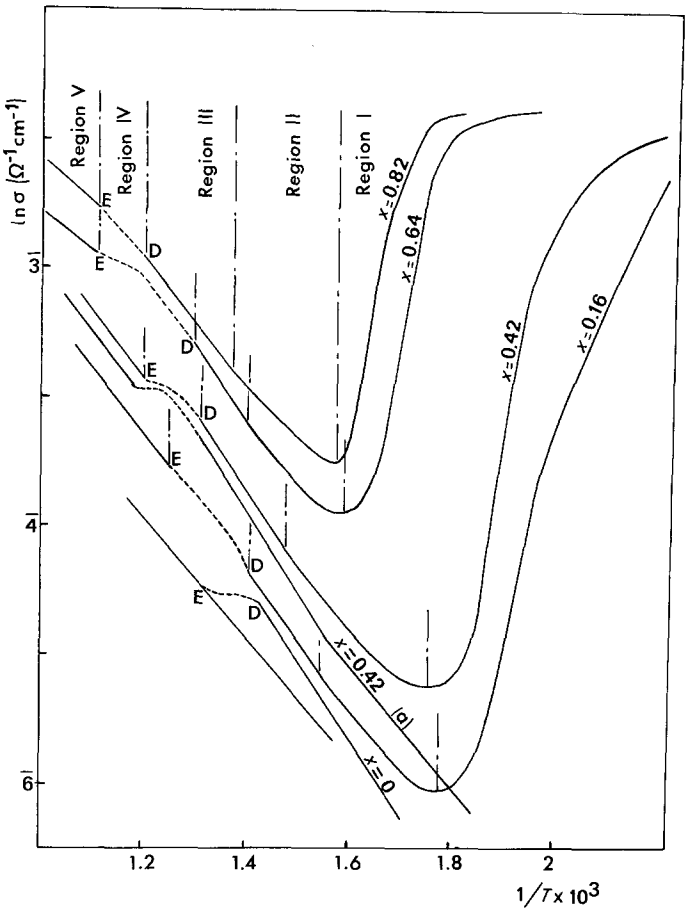

Figure 3 Behaviour of electrical conductivity during the transformation of initial phase → γ-phase → α-phase; cobalt substituted magnetites.

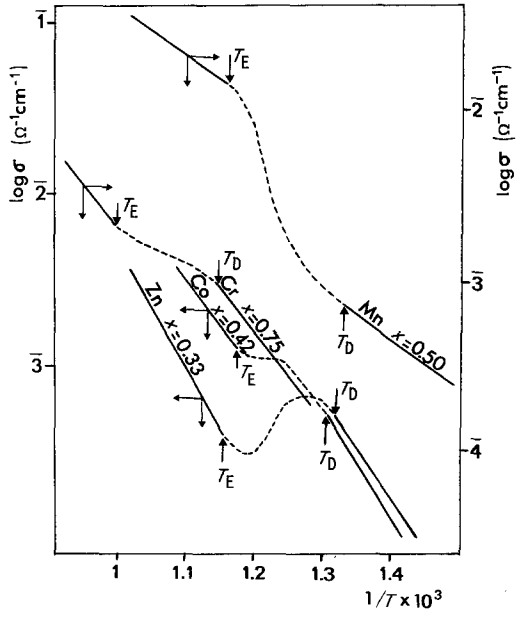

Figure 4 Effect of divalent or trivalent cations on the variation of electrical conductivity in the vicinity of the γ → α transformation.

exothermic peak has also been found in the temperature range 500 to 560° C. In this region, a careful analysis of the thermogravimetric (TG) curves indicates a continuous weight gain which probably manifests the oxidation of Mn^{2+} ions not totally oxidized at lower temperatures [15].

The effect of cations on the transformation temperature, T_M, is represented in Fig. 5. Substitution of divalent or trivalent cation increased the precipitation temperature, with manganese ions having a less pronounced effect. For cobalt- and zinc-substituted magnetites, an increase in the precipitation temperature, caused by the decrease in α-Fe_2O_3 concentration, might be closely associated with the cation vacancy in the spinel lattice, since homogeneous oxidation of ferrous ferrites generates cation vacancies on octahedral sites, resulting in the structure

$$(M_x^{2+}Fe_{(8-2x)/3}^{3+}\square_{(1-x)/3})O_4^{2-} \quad 0 < x < 1.$$

These γ phases are converted to α phases according to the reaction:

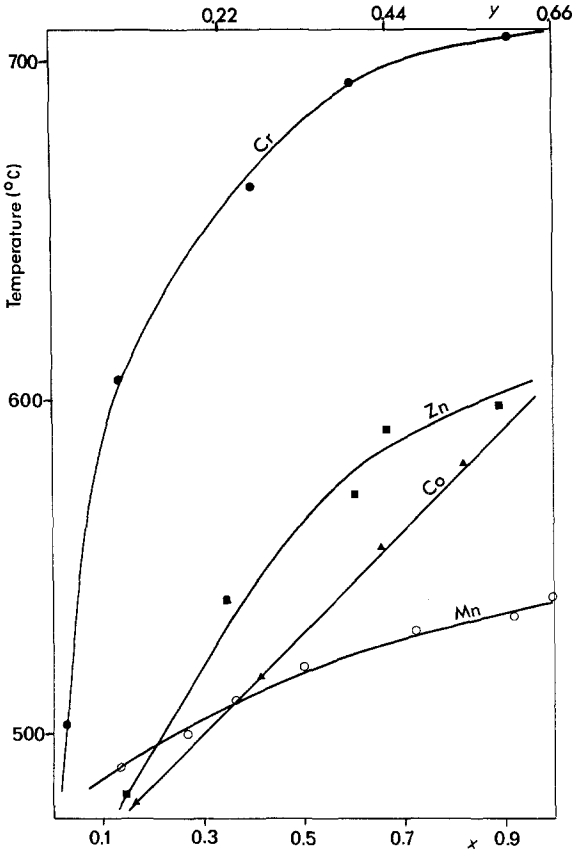

Figure 5 Variation of T_M with composition for different spinels.

$$(M^{2+}_{3x}Fe^{3+}_{8-x}\square_{1-x})O^{2-}_{12} \rightarrow 3x\,Zn^{2+}Fe^{3+}_2O^{2-}_4 + 4(1-x)Fe^{3+}_2O^{2-}_3.$$

The concentration of vacancies is thus proportional to the α-Fe_2O_3 content. In the case of aluminium- or chromium-substituted magnetites, the α-phase composition is the same as that of the γ-phase which may be considered as being written:

$$(Fe^{3+}_{(8-8y)/3}M^{3+}_{8y/3}\square_{1/3})O^{2-}_4 \quad 0<y<2/3;$$

and for manganese-substituted magnetite:

$$(Fe^{3+}_{(8-3x)/3}Mn^{3+}_x\square_{1/3})O^{2-}_4 \quad 0<x<1.$$

The concentration of vacancies generated after oxidation is constant with composition. Since the same concentration of vacancies for precipitation is observed for different substitution extents, the effect of vacancies on the stabilization of the $\gamma \rightarrow \alpha$ transition may not explain the increase in stability with substitution extent.

The stabilization of the spinel solid solution by the distribution cation could also be considered. An earlier paper [5] showed that the process proposed by Kachi *et al.* [16] for the restacking of γ-Fe_2O_3 to α-Fe_2O_3 may be assumed valid for all substituted magnetites. The final process consisting of transforming the "kagome" lattices formed at the beginning of the transformation into the "honey comb" lattices of the final rhombohedral phase must take those vacancies into account. Under these conditions some metallic ions (Fe^{3+} ions for the restacking for γ-Fe_2O_3 to α-Fe_2O_3) will cooperatively migrate to neighbouring positions and the "honey comb" configuration is set up. Thus, incorporation of different elements as Cr^{3+}, Al^{3+} ions in octahedral sites in the spinel lattice hinder the transformation, because they may suppress the migration of ferric ions to occupy octahedral sites. Furthermore, Mn^{3+} ions do not inhibit the reaction so strikingly as Al^{3+} or Cr^{3+} ions do. In this case, an Mn^{3+} ion created from the oxidation *in situ* of an Mn^{2+} ion may be expected to act as a driving force for the migration.

3.2. Kinetics of haematite precipitation from zinc- or cobalt-substituted defective spinels

As mentioned above, the transformation from defective spinels of the type $[M^{2+}_xFe^{3+}_{(8-2x)/3}\square_{(1-x)/3}]O^{2-}_4$ to corundum-type α-Fe_2O_3 can be directly investigated by evaluating the behaviour of the electrical conductivity in region IV. The transformation degree, α_t, can be defined as:

$$\alpha_t = (\sigma_i - \sigma_t)/(\sigma_i - \sigma_f)$$

where σ_i is the conductivity of the initial phase, σ_t the conductivity at time t, and σ_f the conductivity after transformation.

Fig. 6 shows precipitation isotherms for the zinc-substituted defective spinel for $x = 0.33$ and $x = 0.90$ for a particle size of about 50 nm. An increase in the Fe_2O_3 concentration increases the rate of precipitation as shown in the 499 or 468° C isotherms. These curves can be represented to within the experimental uncertainty by the equation $-\log(1-\alpha_t) = kt^n$ where k is a time-scaling constant and n a constant determining curve shape (exponential if $n = 1$, sigmoidal if $n > 1$). While the data are best described by an exponential equation with $n = 1$ for $x = 0.90$ which implies diffusion-controlled growth, the data at the lower extent ($x = 0.33$) are consistent with a sigmoidal law indicating that the process could be nucleation-controlled. An Arrhenius plot

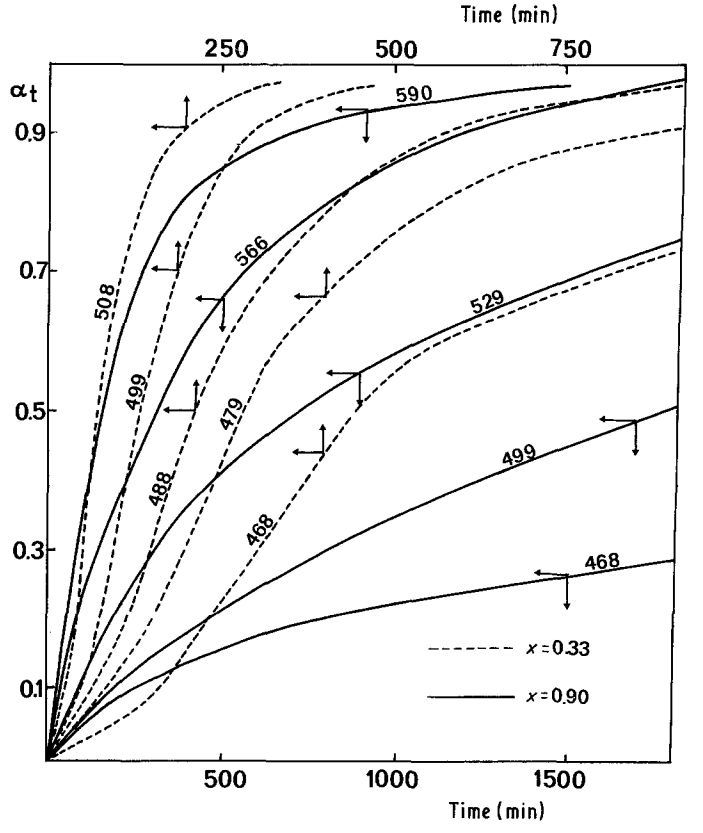

Figure 6 Precipitation isotherms for zinc-substituted defective spinels.

of the constant k against the reciprocal temperature gave the activation energy. As examples, the activation energies for $x = 0.90$ and $x = 0.33$ were calculated as 38 and 49 kcal mol^{-1}, respectively. Similar results have been found for cobalt-substituted magnetites with activation energies of 37 kcal mol^{-1} for $x = 0.82$ and 51.7 kcal mol^{-1} for $x = 0.16$. The reported values for the transformation γ-$Fe_2O_3 \rightarrow \alpha$-$Fe_2O_3$ show a large spread, from a minimum of 36.6 kcal mol^{-1} to a maximum of 86 kcal mol^{-1} [16, 17]. This failure to obtain consistent results has been attributed, among other factors, to the presence of impurities [17], and to the influence of particle size [18]. In this case, Feitknecht and Mannweiler [18] proposed that γ-Fe_2O_3 with particle size of about 50 nm transforms to α-Fe_2O_3 by a nucleation mechanism and that γ-Fe_2O_3 with particle size of more than 70 nm, transforms by a slow growth of the nuclei. Evidence supporting this assumption can be found in Fig. 7 which illustrates the kinetic curves for two different particle sizes. The transformation is shown to proceed by diffusion-controlled growth for a particle size of 92 nm and by nucleation as a significant process for a particle size of about 50 nm. Furthermore, the rate of precipitation increased with increasing particle size. This confirms that an increase in particle size facilitates the formation of α-Fe_2O_3.

4. Conclusion

The results obtained in this study are:

1. the behaviour of the electrical conductivity of "cubic" iron sesquioxides, γ-Fe_2O_3, substituted by divalent or trivalent ions was discussed, especially during transformation to the rhombohedral phases;

2. in the case of γ-$Fe_2O_3 \rightarrow \alpha$-$Fe_2O_3$ transformation, the effects of particle size and oxidation extent were studied. It was found that the reduced particle size facilitates the release of strain which increases the transformation temperature, and that the lower the percentage of γ-Fe_2O_3 in solid solution Fe_3O_4–γ-Fe_2O_3, the higher the temperature of the $\gamma \rightarrow \alpha$ transformation.

3. the effects of substitution extent and divalent or trivalent cation were also studied. The temperature, T_M, related to temperatures T_D and T_E at the beginning and the end of each discontinuity by $T_M = (T_D + T_E)/2$, increase with increase in

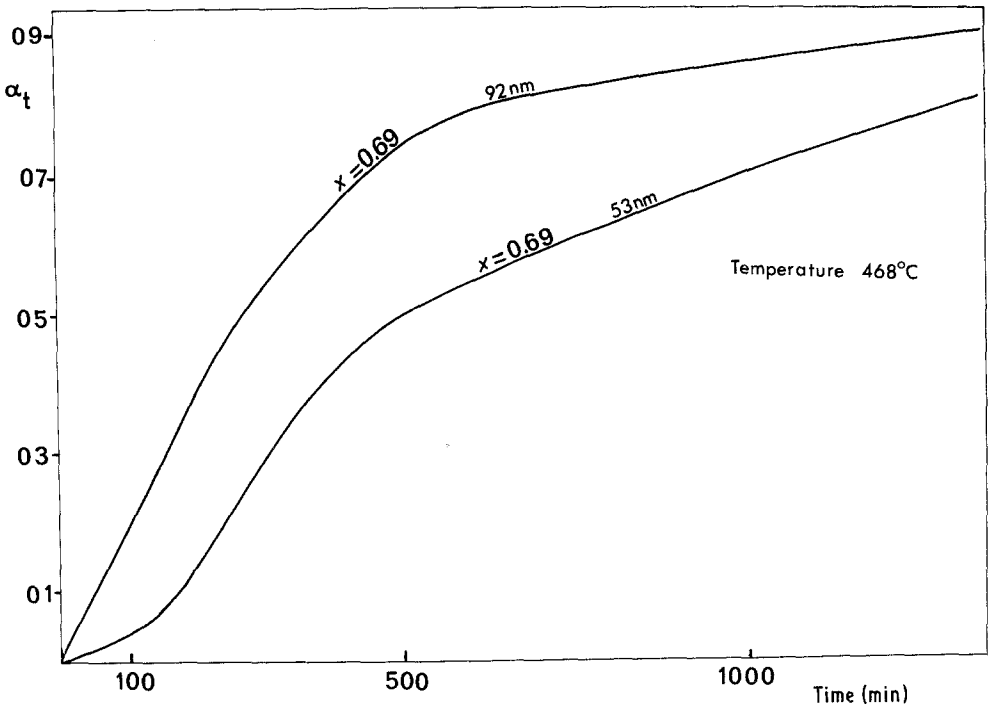

Figure 7 Effect of particle size on the rate of precipitation.

substitution extent. Stabilization of spinel solid solution by the cation is more pronounced for zinc and cobalt than for manganese;

4. the kinetics for haematite precipitation from divalent substituted defective spinels can be directly investigated by following the variation of electrical conductivity in the discontinuity region. The experimental data show that the transformation can be described according to the equation $-\log(1-\alpha) = kt^n$ with $n = 2.4$ for $x = 0.33$ or $x = 0.16$ and $n = 1$ for $x = 0.90$ or $x = 0.82$. At constant temperature, an increase in the γ-Fe_2O_3 concentration increases the rate of haematite precipitation.

References

1. B. GILLOT, F. CHASSAGNEUX and A. ROUSSET, *Mater. Chem.* 6 (1981) 233.
2. B. GILLOT, F. BOUTON, F. CHASSAGNEUX and A. ROUSSET, *J. Solid State Chem.* 33 (1980) 245.
3. B. GILLOT, R. M. BENLOUCIF and A. ROUSSET, *ibid.* 39 (1981) 329.
4. B. GILLOT, A. ROUSSET and G. DUPRE, *ibid.* 25 (1978) 263.
5. B. GILLOT, *Mater. Res. Bull.* 13 (1978) 783.
6. B. GILLOT, F. JEMMALI and A. ROUSSET, *J. Solid State Chem.* 50 (1983) 138.
7. Y. NAKATANI and M. MATSUOKA, *Jap. J. Appl. Phys.* 22 (1983) 233.
8. A. ROUSSET, P. GERMI and J. PARIS, *Ann. Chim. Fr.* 7 (1972) 57.
9. P. MOLLARD, A. COLLOMB, J. DEVENYI, A. ROUSSET and J. PARIS, *IEEE Trans. Mag.* **Mag11** (1975) 894.
10. F. CHASSAGNEUX and A. ROUSSET, *J. Solid State Chem.* 16 (1976) 161.
11. B. GILLOT and J. F. FERRIOT, *J. Phys. Chem. Solids* 37 (1976) 857.
12. K. EGGER and W. FEITKNECHT, *Helv. Chim. Acta* 45 (1962) 2042.
13. K. KIMURA, S. OHISHI and T. YAMAGUCHI, *J. Amer. Ceram. Soc.* 62 (1979) 533.
14. B. GILLOT, R. M. BENLOUCIF and A. ROUSSET, *Phys. Status Solidi (a)* 65 (1981) 205.
15. B. GILLOT and A. ROUSSET, *Compt. Rend. Acad. Sci.* 299 (1984) 231.
16. S. KACHI, K. MOMIYAMA and S. SHIMIZU, *J. Phys. Soc. Japan* 18 (1963) 106.
17. F. E. de BOER and P. W. SELWOOD, *J. Amer. Chem. Soc.* 76 (1954) 3365.
18. W. FEITKNECHT and U. MANNWEILER, *Helv. Chim. Acta* 50 (1967) 570.

Received 24 January
and accepted 31 January 1984